

Impacts of Superplasticizers on Rheology and Strength of Alkali-Activated Rock-based Binder

Sajjad Yousefi Oderji*, Pouya Khalili, Mahmoud Khalifeh, Arild Saasen

Dept. of Energy & Petroleum Eng., Faculty of Science and Technology, University of Stavanger, Stavanger, Norway

ABSTRACT

The effect of superplasticizer on rheology and mechanical strength of alkali-activated materials has been one of the issues in terms of selecting a proper superplasticizer. The influence of different superplasticizers (i.e., potassium silicates, borax, lignosulfonate) on the rheology and strength of alkali-activated rock (norite-based) binder cured under room temperature have been studied. Initially, mini-slump flow test and strength development of the control sample and the slurry containing these superplasticizers was measured. Compressive strength tests were conducted to determine the superplasticizers effects on the hardened properties of the binders. The advantages and shortcomings of different used superplasticizers on fresh and hardened properties of alkali-activated norite-based binder cured under ambient condition were evaluated. Based on the obtained results, viscosity, yield stress, zeta potential, and consistency of the top candidate was studied. Na-lignosulfonate significantly reduced the yield stress and increased flowability; however, the potassium silicates showed the least impact on the yield stress and flowability.

Keywords: Superplasticizer, Alkali-activated material, Geopolymer, Rheology, Compressive strength, Mining waste, Norite, Rock-based.

INTRODUCTION

After water, concrete is the most used material on the earth^{1,2}. Ordinary Portland Cement (OPC) is used as paste to produce concrete³. However, the OPC production is one of the largest sources of carbon dioxide (CO₂) emission, and it is responsible for approximately 5–7% of total global CO₂ emission into the atmosphere^{4,5}. Therefore, an alternative cementation materials to OPC, which can reduce the carbon footprint of cement production have leverage⁶. This has encouraged researchers to develop environmentally friendly alternatives such as alkali activated materials and geopolymers^{7,8}.

Alkali-activated materials (AAMs), including geopolymers (GPs), due to their advantages such as applicability to utilize wastes and byproducts are growing as an important alternative for cement^{9,10}. Besides, utilization of these materials significantly reduces the CO₂ emissions, it helps to reduce the negative environmental consequences of waste land-filling issues^{11,12}. AAMs and GPs are usually made by synthesise of an aluminum silicate as precursors with an alkaline activator, such as potassium hydroxide (KOH), sodium hydroxide (NaOH), potassium silicate (K₂SiO₃), sodium silicate (Na₂SiO₃) or combination of them^{3,7}.

The geopolymerization process contains of the following steps:(i) dissolution of the aluminosilicate solids in the alkaline aqueous solution, (ii) transportation of ions, (iii) formation and nucleation of oligomeric consisting of Si–O–Si/Si–O–Al, (iv) polycondensation of the oligomers to build up a three-dimensional aluminosilicate network and finally (v) hardening by cross-linking of the whole system into a polymeric structure thorough bonding of the undissolved solid particles into an established network. The empirical formula of the poly(sialate) is as¹³: $M_n \{-(SiO_2)_z-AlO_2\}_n \cdot wH_2O$; where M is a cation such as K⁺, Na⁺ or Ca²⁺, n is a degree of polycondensation, and z is 1,2 ,3 or higher.

S. Y. Oderji et al.

Mechanical strength and rheological behavior are the two most important parameters for evaluating field application of cementitious materials, such as alkali-activated materials and geopolymers^{10,14}. It has been reported that alkali-activated materials and geopolymers are very sensitive to the proportion of added water to the mix¹¹. This is due to chemistry of geopolymerization which does not consume water and production of water molecules as result of reaction. Although using high water content improves the rheology properties, it significantly reduces mechanical strength^{11,15,16}. Therefore, selecting a proper superplasticizer to improve the rheological properties of AAMs and GPs without deteriorating the mechanical strength is important in this field. This will even be more challenging because most chemical admixtures including superplasticizers are being used for OPC-based materials and they are not that effective on alkali-activated materials and geopolymers^{11,17}. These superplasticizers are unstable in high pH environments and their adsorption rate on non-calcium particles is low¹⁸. Experimental results shows that superplasticizers with chemical structure like surfactants, with sufficient stability in high pH medium, are potential candidates¹⁹.

This research work aims to identify potential admixtures as superplasticizer and initially investigating their effect on flowability and compressive strength of alkali-activated rock (norite)-based binder. Compressive strength tests were conducted to determine the superplasticizers' effects on the hardened properties of alkali-activated norite-based binders cured at room temperature. Consequently, the top dispersant candidate is selected for further investigation by conducting electrical potential, viscosity, yield stress, and storage and loss moduli measurements.

EXPERIMENTAL PROCEDURE

Materials and Mix proportions

In this study, norite to ground granulated blast-furnace slag (GGBFS) ratio of 80/20 was selected as precursors. The liquid potassium hydroxide (KOH) with a molar ratio of 12 M was used as an alkaline activator, and deionized water as additional water. Six samples were prepared, one as control sample, four samples with different admixtures and one of the samples was made by combination of the two admixtures. The admixtures used in this study are sodium tetraborate decahydrate-Borax(B)-(Na₂B₄O₇·10H₂O), sodium lignosulfonate (L), Potassium silicate (K35T) with Si/K molar ratio of 3.5, and Potassium silicate (K57M) with Si/K molar ratio of 0.98. The selection of silicate solutions and sodium lignosulfonate admixtures was based on their surfactant properties. The 2 wt.% SPs dosage was selected as a baseline for comparison in this research, as some of the used superplasticizers for AAMs and GPs were reported to be most effective around this range^{11,20,21}. However, it should be noted that optimization of the selected SP ratio is not the focus of the current study. The mix proportion of the binders is presented in Table 1. Table 2 presents chemical composition of the precursors determined by the X-ray fluorescence (XRF) analysis²².

Table 1. Mix proportion of the binder in weight %.

Mix Id	Admixture	Norite/ GGBFS Ratio	KOH*	Additional* water	Admixture*
C	-	80/20	20%	20%	-
M	K57M	80/20	20%	20%	2%
K	K35T	80/20	20%	20%	2%
B	Borax	80/20	20%	20%	2%
L	Lignosulfonate	80/20	20%	20%	2%
(K+B)	K35T+Borax	80/20	20%	20%	2%+2%

Notice: *Activator dosage and added water were considered as the mass of precursors (%).

Table 2. Chemical composition of Norite and GGBFS (% by mass).

oxides	SiO ₂	Al ₂ O ₃	CaO	MgO	Fe ₂ O ₃	Na ₂ O	K ₂ O	TiO ₂	MnO	Mn ₂ O ₃	S ²⁻	Cr ₂ O ₃	SO ₃	P ₂ O ₅	LOI
Norite	43	15.5	6.6	6.8	12.5	3.4	0.9	8.2	0.1	0.1	0.3	0.03	0.1	0.3	2.57
GGBFS	34	13	31	17	0.42	0.27	0.26	2.4	0.17	0.6	1.1	-	-	-	-

Mixing procedure and testing

Norite and GGBFS were dry mixed in a Hobart planetary mixer for 2 minutes at the lowest speed rate (1). Afterwards, the liquid alkali activator and deionized water were introduced, and the mixing was continued for 3 minutes with the same speed. Subsequently, the admixture was added and mixed for 2 more minutes at the same speed. In the end, the mixer was stopped for 30 second for cleaning the paste, which is adhered to the mixer with spatula. In the final stage, the mixer is run at the highest speed (3) for 2.5 minutes. When the mixing process was completed, the pastes were casted into 50×100 mm cylindrical molds and vibrated for 1 minute to minimize presence of air bubbles. The specimens were demolded after 24h and kept in the curing room with a temperature of 20±3°C until the compressive strength testing took place.

To determine the flowability of the mix designs, flow table test was conducted to measure the flowability of pastes. Compressive strength tests were conducted at a loading rate of 7 N/s using an MTS servo hydraulic testing machine according to the ASTM C109 standard. Atmospheric consistometer (Model 60-OFITE) was utilized to obtain the thickening time of paste to investigate the rheology of pastes further. Anton Paar MCR 302 rheometer was used to measure the rheological parameters of the mix designs. In both rotational and oscillatory tests, concentric cylinder measuring system was used due to particle size concerns. The Electrophoretic Light Scattering (ELS) using a Zetasizer Nano ZS (Malvern) equipped with a laser source (wavelength 633 nm) at a scattered angle of 13° was used for Zeta potential measurements.

RESULTS AND DISCUSSION

Influence of different admixture on the flowability

Effect of the admixtures on the flowability was measured through mini-slump tests, given in Fig. 1. As shown in the Figure, sodium lignosulfonate significantly increased the flowability. However, application of the lignosulfonate prolonged the setting time. Ren et al.²¹ reported the same behavior with adding sodium lignosulfonate to alkali-activated slags. In other study, Luukkonen et al.¹⁷ investigated the effects of lignosulfonate on alkali-activated slag-based materials. They found lignosulfonate caused the lignin chains and consequently the steric repulsion between particles. Other research by Palacios et al.²³ studied the adsorption of some superplasticizers on alkali-activated slag pastes. They claimed that the effective superplasticizer in their research works because of its structural stability in high alkaline media. Those statements might be the reason sodium lignosulfonate worked in our study.

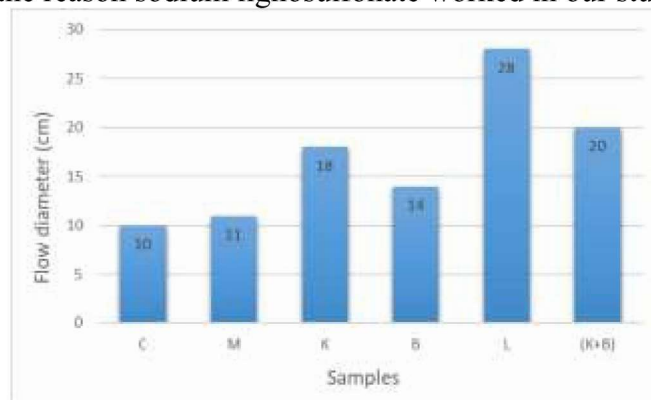


FIGURE 1: The influence of different admixtures on flowability of alkali-activated Norite-based.

Influence of different admixture on the compressive strength (UCS)

The 3-day compressive strength results of alkali-activated norite-based binder with 2% of different admixtures are shown in Fig. 2. The binders with sodium lignosulfonate (L) as admixture increased compressive strength of binders compared to control sample (C). The possible reasoning might be the participation of sodium in the chemical reaction. According to literature, the chelating effect of lignosulfonate, which increases strongly at high pH, has likely contributed to improve setting time and also compressive strength^{17,24}.

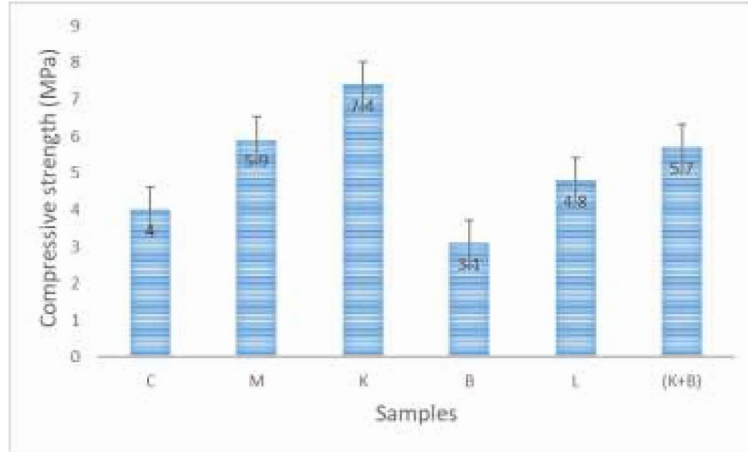


FIGURE 2: Influence of different admixtures on compressive strength (3-d).

Rheological behavior

Flow curve

To understand the rheological behavior of the mix designs, further investigation took place on control paste (denoted by C) and the paste with lignosulfonate selected (denoted by L). Alkali-activated materials are a viscoelastic material, which means it shows viscous and elastic behavior at the same time. In the first step, a rotational viscometry test with a controlled shear rate was performed on the pastes (C and L). Figs. 3 and 4 show the flow curve of the control sample and the sample containing the lignosulfonate as superplasticizer, respectively. Table 3 shows the rheological parameters calculated for these measurements using two different rheological models. Bingham model (Equation 1) is presented as follows:

$$\tau = \tau_y + \mu_p \dot{\gamma} \quad (1)$$

where τ is the shear stress, τ_y is the Bingham yield stress, μ_p is the plastic viscosity and $\dot{\gamma}$ is the shear rate. Herschel-Bulkley is a three-parameter viscosity model which has the ability to reasonably fitting flow curves of fluids showing shear-dependent viscosity^{25,26}. This model is shown as (Equation 2):

$$\tau = \tau_y + k\dot{\gamma}^n, \tau > \tau_y \quad (2)$$

where k is the consistency index, τ_y is the yield stress and n is the flow behavior index, which is an indication of the different flow behavior of fluid ($n < 1$ shear thinning, $n > 1$ shear thickening, and $n = 1$ Newtonian). In very low shear rates ($4\text{-}20 \text{ s}^{-1}$), sample C had higher shear stress in the ramp down profile compared to the ramp up. Usually, such behavior is rooted from particle sedimentation or chemical reaction resulting in gel development. The viscosity function is also shown in Fig. 5 representing the shear-thinning behavior of the control sample (C). However, the sample L exhibited two different behavior, shear-thinning at low shear rates and Bingham behavior at high shear rates. Considering civil engineering applications and 3D printing, the shear rates above 10 s^{-1} may not be applicable for the field; however, it can be of interest for other applications such as well construction.

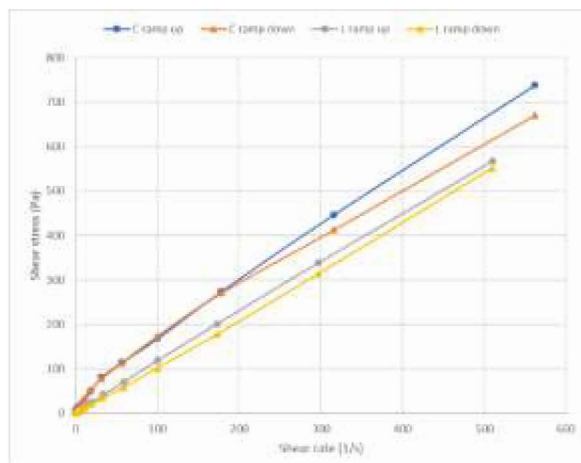


FIGURE 3: Flow curve of the control sample (C) and sample contains lignosulfonate (L), covering full shear rate ranges.

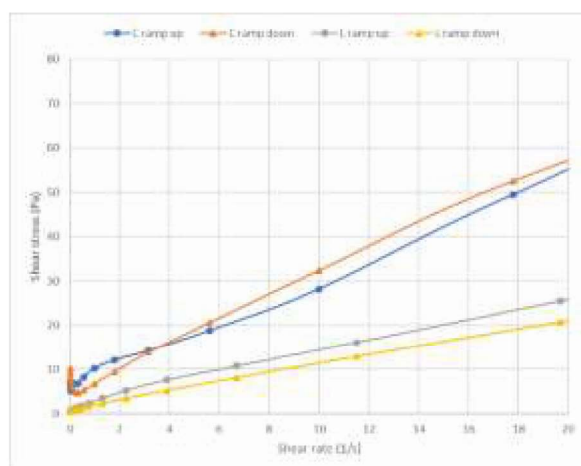


FIGURE 4: Flow curve of the control sample (C) and sample contains lignosulfonate (L), covering low shear rate ranges.

Table 3. rheological parameters of the control sample (C) and the sample contains lignosulfonate (L).

Model functions	Parameters	Sample C	Sample L
Herschel-Bulkley	Flow behavior index (n)	0.57849	1.0233
	Yield stress (Pa)	8,05	2.4397
	Consistency index ($Pa \cdot s^n$)	12.777	0.9638
Bingham	Yield stress (Pa)	4.9841	0.56249
	Infinite shear viscosity (mPa.s)	1883.8	1124.9

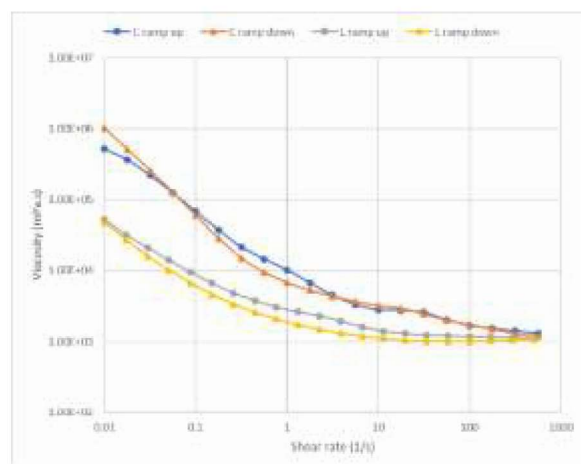


FIGURE 5: Viscosity of the sample(C) and the sample contains lignosulfonate(L) in log-log scale.

Oscillatory test

Effects of the lignosulfonate on the viscoelasticity of the paste, shear strain amplitude sweep with a constant frequency of 10 rad/s was conducted on the samples at room temperature (see Figs. 6 and 7). Before conducting the test, samples were pre-mixed for 30 sec at 100 1/s, followed by a 2 min resting time. The G' (storage modulus) is the energy that material stores when it gets deformed, and later it uses this energy to get back to its initial structure. Hence, it is an indication of the elastic portion of the material. The G'' (loss modulus), on the other hand, is an indication of the viscous behavior of the material when deformation occurs and represents the energy that is lost due to internal friction between particles and molecules.

In the LVE (linear viscoelastic) region, G' is higher than G'' which means elastic behavior dominates the viscous one, and paste shows a gel character. Within the LVE range, the material structure is preserved, and immediately after exiting this range, the material structure experiences permanent changes, and particles may slowly leap-frog. This critical point is usually called the yield point. When G' becomes equal and lower than G'' , the paste started to flow and it switches to the liquid state. This point is known as flow point ²⁷. The strain and shear stress at the flow point were 1.491% and 2.536 Pa for the control sample and 0.2332 % and 0.1612 Pa for the sample with the sodium lignosulfonate. Storage modulus is in the order of 10000 and 1000 for the control and the sample with sodium lignosulfonate, respectively.

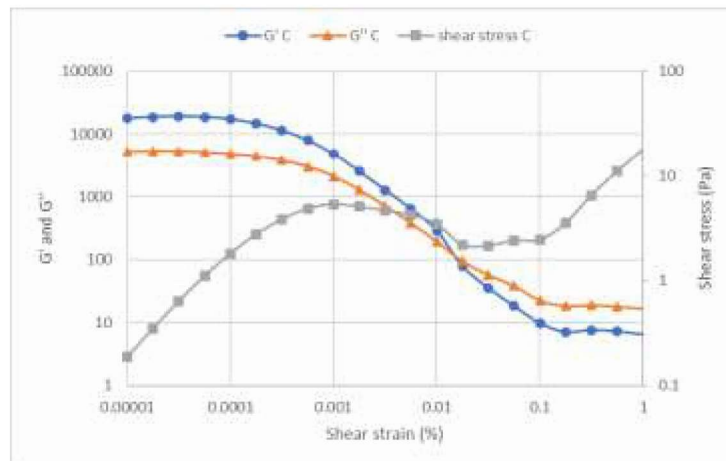


FIGURE 6: Amplitude sweep test of control sample (C).

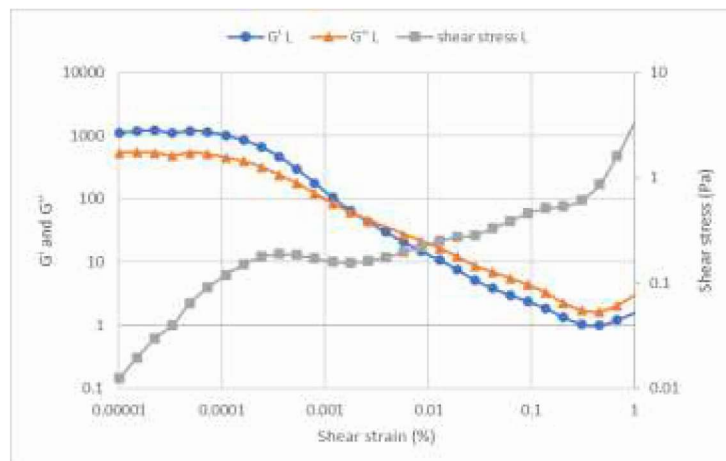


FIGURE 7: Amplitude sweep test of the sample with lignosulfonate (L).

Zeta potential

The higher absolute value of zeta potential shows the higher electrostatic repulsion effect²⁸. Zeta potential measured for these samples showed -24.6 mV for the control sample and -32.4 mV for the sample that contains lignosulfonate. The reduction in zeta potential value means admixture is effectively adsorbed on the particle surface and results in a high negative electric charge, which causes the particles to repel each other. Thus, resulting in a more stable system^{14,29}. The lower absolute value of zeta potential of the control sample can be correlated to the higher flow point of sample since this sample tends to have more agglomerated particles at conditions close to resting. By increasing the shear strain to a certain value, which is 1.491% here, the agglomerates fall apart, and the paste was free to flow. The zeta potential measurement was conducted straight after mixing and stability of the dispersant in the alkaline medium was a question. Therefore, consistency experiment could help to find out the answer. The zeta potential shows the electric double layer forces between particles, and it has a direct relationship to yield stress¹⁸. The result of this research is in line with other study, which showed an increase in the absolute zeta potential value could reduce the yield stress¹⁸.

Consistency results

Fig. 8 shows the time-dependent functions of G' and G'' for the sample L. During this test time frame, the temperature was kept constant, and the sample oscillated with constant shear strain chosen from the LVE range. The consistency of the pastes was measured using a consistometer, which is designed for oil and gas industry. This device has a container that is filled with paste and is rotated at a constant rate and the torque that the paste imposes is measured. The paste container is placed inside an oil bath to control the temperature. Fig. 9 shows the thickening time of pastes measured in Bearden Consistency Units (Bc) at room temperature. In oil cementing operation, 40 Bc is regarded as a value beyond which the slurry is unpumpable³⁰. However, in this study the materials design was developed for construction applications. The consistency data shows the dissolution and oligomerization phases, see Fig. 9. Use of lignosulfonate increased the dissolution rate and prolonged the oligomerization phase. This should result in higher compressive strength that is aligned with measured UCS data. In addition, the consistency data indirectly shows that dispersant is stable, up to 120 minutes, in the alkaline environment.

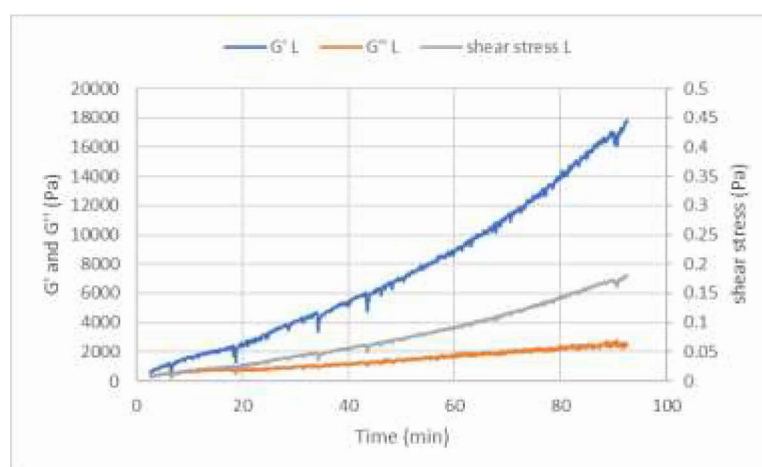


FIGURE 8: Time-dependent viscoelasticity of the sample contains lignosulfonate.

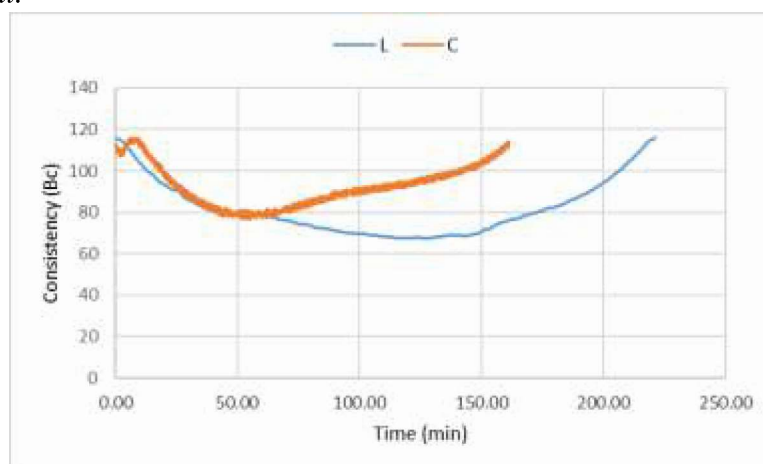


FIGURE 9: Thickening time of the control sample and the sample contains lignosulfonate.

Conclusion

The effect of different admixtures as superplasticizer on alkali-activated norite binders were evaluated. Flowability and compressive strength of the slurries containing these admixtures were measured. The best admixtures candidate was selected for further investigation. Zeta potential, viscosity, yield stress, and consistency of the samples were evaluated. The results showed that the sodium lignosulfonate had positive results on the improvement of rheology behavior and strength of norite-based binders cured at ambient temperature. Therefore, it can be concluded that samples with sodium lignosulfonate were deemed to have better performance in terms of workability and compressive strength properties. Moreover, adding sodium lignosulfonate to alkali-activated norite-based binders resulted in higher absolute value of zeta potential. Colloidal interactions after introducing sodium lignosulfonate caused lower yield stress of paste.

Acknowledgment:

The authors would like to thank the research council of Norway (RCN) and Saferock AS for financially funding the project titled " Geopolymer concrete based on mining residues-SolidRock", RCN# 321486.

References:

1. Makul N. Advanced smart concrete-A review of current progress, benefits and challenges. *J Clean Prod.* 2020;274:122899.
2. Meena K, Luhar S. Effect of wastewater on properties of concrete. *J Build Eng.* 2019;21:106-112.
3. Khalifeh M, Saasen A, Vrålstad T, Larsen HB, Hodne H. Experimental study on the synthesis and characterization of aplite rock-based geopolymers. *J Sustain Cem Mater.* 2016;5(4):233-246.
4. Shah SFA, Chen B, Oderji SY, Haque MA, Ahmad MR. Improvement of early strength of fly ash-slag based one-part alkali activated mortar. *Constr Build Mater.* 2020;246:118533.
5. Naqi A, Jang JG. Recent progress in green cement technology utilizing low-carbon emission fuels and raw materials: A review. *Sustainability.* 2019;11(2):537.
6. Khalifeh M, Saasen A, Vrålstad T. Potential utilization of geopolymers in plug and abandonment operations. In: *SPE Bergen One Day Seminar.* OnePetro; 2014.
7. Oderji SY, Chen B, Jaffar STA. Effects of relative humidity on the properties of fly ash-based geopolymers. *Constr Build Mater.* 2017;153:268-273.
8. Khalifeh M, Saasen A, Hodne H, Godøy R, Vrålstad T. Geopolymers as an alternative for oil well cementing applications: A review of advantages and concerns. *J Energy Resour Technol.* 2018;140(9).
9. Lazorenko G, Kasprzhitskii A. Geopolymer additive manufacturing: A review. *Addit Manuf.* Published online 2022:102782.

10. Oderji SY, Chen B, Ahmad MR, Shah SFA. Fresh and hardened properties of one-part fly ash-based geopolymer binders cured at room temperature: Effect of slag and alkali activators. *J Clean Prod.* 2019;225:1-10.
11. Oderji SY, Chen B, Shakya C, Ahmad MR, Shah SFA. Influence of superplasticizers and retarders on the workability and strength of one-part alkali-activated fly ash/slag binders cured at room temperature. *Constr Build Mater.* 2019;229:116891.
12. Khalifeh M, Motra HB, Saasen A, Hodne H. Potential utilization for a rock-based geopolymer in oil well cementing. In: *International Conference on Offshore Mechanics and Arctic Engineering.* Vol 51296. American Society of Mechanical Engineers; 2018:V008T11A037.
13. Davidovits J, Orlinski J. '99 *Geopolymer International Conference Proceedings.* Geopolymer Institute; 1999.
14. Lu C, Zhang Z, Shi C, Li N, Jiao D, Yuan Q. Rheology of alkali-activated materials: A review. *Cem Concr Compos.* 2021;121:104061.
15. Pnias D, Giannopoulou IP, Perraki T. Effect of synthesis parameters on the mechanical properties of fly ash-based geopolymers. *Colloids Surfaces A Physicochem Eng Asp.* 2007;301(1-3):246-254.
16. Xie J, Kayali O. Effect of initial water content and curing moisture conditions on the development of fly ash-based geopolymers in heat and ambient temperature. *Constr Build Mater.* 2014;67:20-28.
17. Luukkonen T, Abdollahnejad Z, Ohenoja K, Kinnunen P, Illikainen M. Suitability of commercial superplasticizers for one-part alkali-activated blast-furnace slag mortar. *J Sustain Cem Mater.* 2019;8(4):244-257.
18. Kashani A, Provis JL, Qiao GG, van Deventer JSJ. The interrelationship between surface chemistry and rheology in alkali activated slag paste. *Constr Build Mater.* 2014;65:583-591.
19. Hjelm, S. 2022. Revealing the Effect of Superplasticizers on Viscosity and Yield Stress of Geopolymers. Bachelor project a Dept. of Energy and Petroleum Eng., University of Stavanger, Spring 2022.
20. Cheng Y, Cong P, Hao H, et al. Improving workability and mechanical properties of one-part waste brick power based-binders with superplasticizers. *Constr Build Mater.* 2022;335:127535.
21. Ren J, Bai Y, Earle MJ, Yang C. A preliminary study on the effect of separate addition of lignosulfonate superplasticiser and waterglass on the rheological behaviour of alkali-activated slags. In: *Third International Conference on Sustainable Construction Materials & Technologies (SCMT3), Kyoto, Japan.* ; 2013:1-11.
22. Khalifeh M, Saasen A, Larsen HB, Hodne H. Development and characterization of norite-based cementitious binder from an ilmenite mine waste stream. *Adv Mater Sci Eng.* 2017;2017.
23. Palacios M, Houst YF, Bowen P, Puertas F. Adsorption of superplasticizer admixtures on alkali-activated slag pastes. *Cem Concr Res.* 2009;39(8):670-677.
24. Pang YX, Qiu XQ, Yang DJ, Lou HM. Influence of oxidation, hydroxymethylation and sulfomethylation on the physicochemical properties of calcium lignosulfonate. *Colloids Surfaces A Physicochem Eng Asp.* 2008;312(2-3):154-159.
25. Saasen A, Ytrehus JD. Viscosity models for drilling fluids—Herschel-bulkley parameters and their use. *Energies.* 2020;13(20):5271.
26. Saasen A, Ytrehus JD. Rheological properties of drilling fluids: use of dimensionless shear rates in herschel-bulkley and power-law models. *Appl Rheol.* 2018;28(5).
27. Mezger T. *The Rheology Handbook: For Users of Rotational and Oscillatory Rheometers.* European Coatings; 2020.
28. Plank J, Hirsch C. Impact of zeta potential of early cement hydration phases on superplasticizer adsorption. *Cem Concr Res.* 2007;37(4):537-542.
29. Nägele E, Schneider U. The zeta-potential of blast furnace slag and fly ash. *Cem Concr Res.* 1989;19(5):811-820.
30. Kamali M, Khalifeh M, Saasen A, Godøy R, Delabroy L. Alternative setting materials for primary cementing and zonal isolation—Laboratory evaluation of rheological and mechanical properties. *J Pet Sci Eng.* 2021;201:108455.